DMD Fast Forward. Published on April 2, 2007 as doi:10.1124/dmd.107.015396

Effect of arylamine acetyltransferase *Nat3* gene knockout on *N*-acetylation in the mouse

K.S. Sugamori, D. Brenneman, S. Wong, A. Gaedigk[1], V. Yu[2], H. Abramovici[3], R. Rozmahel[4], and D.M. Grant

Department of Pharmacology, Faculty of Medicine
University of Toronto
Toronto, Canada M5S 1A8

DMD Fast Forward. Published on April 2, 2007 as DOI: 10.1124/dmd.107.015396
This article has not been copyedited and formatted. The final version may differ from this version.

Running Title: Arylamine *N*-acetyltransferase *Nat3*(-/-) knockout mice

Corresponding Author: Denis M. Grant, Ph.D.
Department of Pharmacology
University of Toronto
Medical Sciences Building
1 King's College Circle
Toronto, Ontario M5S 1A8
Telephone: 416-978-4653
Fax: 416-978-6395
Email: denis.grant@utoronto.ca

Number of Text Pages: 17

Number of Tables: 2

Number of Figures: 4

Number of References: 40

Number of Words in Abstract: 250

Number of Words in Introduction: 779 (including in-text references)

Number of Words in Discussion: 1292 (including in-text references)

List of Abbreviations: ABP, 4-aminobiphenyl; AABP, *N*-acetyl-4-aminobiphenyl; AF, 2-aminofluorene; AAF, *N*-acetyl-2-aminofluorene; 5-AS, 5-aminosalicylic acid; AUC, area under the curve; DME, drug metabolizing enzyme; ES, embryonic stem; NAT, *N*-acetyltransferase; PAS, *p*-aminosalicylic acid; APAS, *N*-acetyl-PAS; SMZ, sulfamethazine; ASMZ, *N*-acetyl-SMZ.

ABSTRACT

Arylamine *N*-acetyltransferases (NATs) catalyze the biotransformation of many important arylamine drugs and procarcinogens. NATs can either detoxify or activate procarcinogens, complicating the manner in which these enzymes may participate in enhancing or preventing toxic responses to particular agents. Mice possess three NAT isoenzymes, Nat1, Nat2 and Nat3. While Nat1 and Nat2 can efficiently acetylate many arylamines, few substrates appear to be appreciably metabolized by Nat3. We generated a *Nat3* knockout mouse strain and used it along with our double *Nat1/2*(-/-) knockout strain to further investigate the functional role of Nat3. *Nat3*(-/-) mice showed normal viability and reproductive capacity. Nat3 expression was very low in wild-type animals and completely undetectable in *Nat3*(-/-) mice. In contrast, greatly elevated expression of Nat3 transcript was observed in *Nat1/2*(-/-) mice. We used a transcribed marker polymorphism approach to establish that the increased expression of Nat3 in *Nat1/2*(-/-) mice is a positional artifact of insertion of the PGK-*neomycin* resistance cassette in place of the *Nat1/Nat2* gene region and upstream of the intact *Nat3* gene, rather than a biological compensatory mechanism. Despite the increase in Nat3 transcript, the *N*-acetylation of *p*-aminosalicylate, sulfamethazine, 2-aminofluorene and 4-aminobiphenyl was undetectable either *in vivo* or *in vitro* in *Nat1/2*(-/-) animals. In parallel, no difference was observed in the *in vivo* clearance or *in vitro* metabolism of any of these substrates between wild-type and *Nat3*(-/-) mice. Thus Nat3 is unlikely to play a significant role in the *N*-acetylation of arylamines either in wild-type mice or in mice lacking Nat1 and Nat2 activities.

Genetic variation in drug metabolism has been extensively studied as an important factor in determining interindividual susceptibility to environmental toxicant exposure (Nebert, 2000). The arylamine *N*-acetyltransferases (NATs) mediate the acetylation of clinically relevant drugs and procarcinogenic chemicals with homo- and heterocyclic amine structures. Two isoforms, NAT1 and NAT2, are found in humans and are characterized by distinct tissue expression and pharmacological profiles (Grant et al., 2000). While NAT2 has historically been associated with the rapid versus slow acetylator phenotype, the pharmacogenomic revolution has revealed that both NAT1 and NAT2 are highly polymorphic (Boukouvala and Fakis, 2005; Grant et al., 2000). As such, the genetic variation of NATs has been the basis for extensive epidemiological investigations into the role of *NAT* genotypes as modifying risk factors for the development of certain cancers since NATs, paradoxically, can both detoxify and bioactivate procarcinogenic arylamines (Hein, 2002; Hein, 2006).

Metabolic activation by NATs into DNA-binding electrophiles occurs primarily via *O*-acetylation of hydroxylamines, while detoxification into innocuous metabolites is mediated by *N*-acetylation of the parent amine (Hein, 1992), except for diarylamines in which *N*-acetylated DNA adducts are formed (Rothman et al., 1996). *N*-hydroxylation via one or more isoforms of the cytochrome 450s is believed to be the first step in the bioactivation process (Kim and Guengerich, 2005) and may compete with *N*-acetylation in the liver. The nature of the outcome, either activation or detoxification, may be substrate-specific and dependent on the balance of interacting drug metabolizing enzymes (DMEs) that can activate and detoxify procarcinogens, and in particular, on the tissue-specific relative expression of NATs and other DMEs. While epidemiological studies have alluded to a role for NAT acetylator status in altering risk for the development of cancers such as those in colon and bladder, results from these studies are

inconsistent due to differences in sampling size, genotyping procedures, phenotyping/genotyping discordances and exposure situations (for reviews see Boukouvala and Sim, 2005; Hein, 2002; Hein, 2006).

To circumvent some of the problems associated with epidemiological studies in human populations, animal models of acetylation polymorphisms have been used to study the relationship between acetylator phenotype and arylamine-induced indices of toxicity (Hein et al., 1997). In particular, the mouse has been used as a model organism to study the acetylation polymorphism since NAT2 rapid and slow acetylation also occurs in various inbred strains of mice (Glowinski and Weber, 1982). The slow acetylator phenotype is associated with the *Nat2*9* allele found in A/J and A/HeJ mice while rapid acetylator strains, C57BL/6, C3H/HeJ, BALB/c and 129/Ola, carry the *Nat2*8* allele (Boukouvala et al., 2002; Fretland et al., 1997; Kelly and Sim, 1994; Martell et al., 1991). The effect of controlled arylamine exposure on toxic endpoints such as the formation of DNA adducts and tumorigenesis have been investigated using these inbred strains of mice and acetylator congenic mouse strains (Levy and Weber, 1989; Levy and Weber, 1992). However, mouse Nat2 is not functionally equivalent to human NAT2 with respect to substrate-specificity and tissue localization patterns (for review see Boukouvala and Fakis, 2005) thereby confounding the interpretation of these studies in mice.

More recently, the use of gene knockout and transgenic mouse technology has been instrumental for confirming the role of some DMEs in particular toxic responses and for revealing paradoxical responses for other DMEs, thereby contradicting results from some *in vitro* experiments (see Nebert, 2006 for review). These animal models offer the advantage of investigating genetic variation under controlled exposures as well as environmental and secondary genetic influences. We and others have generated knockout mouse models lacking

both *Nat1* and *Nat2* (Sugamori et al., 2003) or *Nat2* alone (Cornish et al., 2003). However, mice possess a third *Nat* gene, *Nat3* (Fretland et al., 1997; Kelly and Sim, 1994). Expression of Nat3 and its polymorphic variants (Boukouvala et al., 2002) in both prokaryotic and eukaryotic expression systems have failed to reveal any prototypical NAT substrates that are efficiently catalyzed by this enzyme. Only a few substrates, namely 5-aminosalicylic acid (5-AS) and 2-aminofluroene (AF), appear to be acetylated by Nat3 at low levels in such systems (Estrada-Rodgers et al., 1998; Kelly and Sim, 1994), and Nat3 mRNA has only been detected in spleen (Boukouvala et al., 2002). Recently, a third *Nat* showing 91% nucleotide identity to mouse *Nat3* has been cloned from rat (Walraven et al., 2006). The rat Nat3, however, can *N*-acetylate a number of substrates including AF, ABP, 5-AS, 3-ethylaniline, 3,5-dimethylaniline, and 4,4'-methylenedianiline, and *O*-acetylate *N*-hydroxy-4-aminobiphenyl. To investigate potential roles or substrates for mouse Nat3, we have generated a *Nat3* knockout mouse model and used it in conjunction with our double knockout *Nat1/2*(-/-) mouse line (Sugamori et al, 2003) to investigate what roles, if any, may be revealed for this enzyme.

DMD Fast Forward. Published on April 2, 2007 as DOI: 10.1124/dmd.107.015396
This article has not been copyedited and formatted. The final version may differ from this version.

MATERIALS AND METHODS

Materials

The pPNT vector was generously provided by Dr. Janet Rossant (Hospital for Sick Children, Toronto, ON, Canada). R1 embryonic stem (ES) cells were from Dr. Andras Nagy (Mount Sinai Hospital, Toronto, ON, Canada). Most ES cell culture reagents (non-essential amino acids, L-glutamine, sodium pyruvate, D-MEM, G418) were purchased from Invitrogen (Burlington, ON, Canada) with the exception β-mercaptoethanol and ganciclovir (Sigma-Aldrich Canada Ltd., Oakville ON, Canada), fetal bovine serum (Hyclone, Logan, UT) and leukaemia inhibitory factor, ESGRO^{TM} (Chemicon International, Inc., Temecula, CA). Acetyl-DL-carnitine, carnitine acetyltransferase, acetyl-CoA sodium salt, PAS, SMZ, ASMZ, ABP, AF and AAF used for NAT activity assays were acquired from Sigma-Aldrich Canada Ltd. APAS was produced in definable quantities from PAS using wild-type recombinant human NAT1 as a catalyst (Dupret et al., 1994) while AABP was generously provided by Dr. M. Novak (Miami University, Oxford, OH). Restriction enzymes for cloning and restriction digests were purchased from Invitrogen. Oligonucleotide primers were synthesized by Invitrogen. CD-1, C57BL/6 (B6), 129/SvJ (129) and CAST/Ei mice were obtained either from Charles River Canada (Saint-Constant, QC, Canada) or The Jackson Laboratory (Bar Harbor, ME). *Nat1/2*(-/-) mice were produced as described (Sugamori et al., 2003). All procedures involving animals were in accordance with the Canadian Council for Animal Care guidelines for use and care of animals.

Construction of targeting vector

A *Nat3* targeting construct was generated using 129/SvJ genomic DNA and the vector pPNT (Tybulewicz et al., 1991), which contains a bacterial phosphoribosyltransferase II gene

conferring neomycin resistance (*neo*) and a herpes simplex virus thymidine kinase (*tk*) gene, each under the transcriptional control of the mouse phosphoglycerate kinase (PGK) promoter. A 6.5 kb *Sac* I/*Kpn* I fragment corresponding to ~ 6 kb of the 5' UTR and 0.48 kb of coding sequence of the *Nat3* 129/SvJ gene was blunt-end ligated into the *Xho* I site of pPNT (see Fig. 1A), located upstream to the bacterial phophoribosyltransferase II gene. A 1.4 kb fragment corresponding to the 3' 0.39 kb of coding sequence and 1 kb of the 3' UTR was generated by PCR (30 cycles of 94°C 10 s, 55°C 10 s, 72 °C, 30 s) using the NAT3/Kpn 5' and 3'primers (see Table 1). This fragment was subcloned into the *Kpn* I site of pPNT located upstream to the *tk* gene. Restriction digests and DNA sequencing confirmed insertion and correct orientation of the sequences. The resulting construct was purified using a QIAGEN MaxiPrep kit (Qiagen Inc., Mississauga, ON).

Production of chimeric mice

R1 embryonic stem (ES) cells were grown in Dulbecco's modified Eagle's medium supplemented with 0.1 mM non-essential amino acids, 1 mM sodium pyruvate, 100 µM β-mercaptoethanol, 2 mM L-glutamine, 20% fetal bovine serum and 1000 U/ml leukaemia inhibitory factor. The plasmid DNA used for targeting was linearized with *Not* I and introduced into early passage R1 ES cells by electroporation (500 µF, 0.24 kV) using a Bio-Rad Gene Pulser II (Bio-Rad Laboratories Ltd., Mississauga, ON, Canada). After selection in medium containing G418 (200 µg/ml) and ganciclovir (2 µM), individual drug-resistant colonies were isolated, expanded and genotyped for the appropriate targeting event (see below). Targeted ES cells were provided to the Transgenic Mouse Facility at the Hospital for Sick Children (Toronto, ON, Canada) for aggregations with CD-1 morulae. A total of 6 male chimeric mice, distinguished by agouti coat color conferred by the R1 ES cells, were generated. Chimeric offspring were crossed

DMD Fast Forward. Published on April 2, 2007 as DOI: 10.1124/dmd.107.015396
This article has not been copyedited and formatted. The final version may differ from this version.

to CD-1 mice to confirm germline transmission by transfer of the agouti coat color. Chimeric males having germline transmission of the targeted ES cells were subsequently crossed with C57BL/6 females, and heterozygotes were intercrossed to produce the homozygous null and wild-type mice used in initial experiments. The homozygous null mice were designated as *Nat3*(-/-). In addition, a congenic C57BL/6 *Nat3*(-/-) line was generated by backcrossing onto the C57BL/6 background for 10 generations. In this case, C57BL/6 mice were used as their wild-type controls.

Genotyping of ES cells and mice

Genomic DNA was isolated from either ES cell clones or mouse tail biopsies. ES cells were lysed overnight at 37˚C in lysis buffer containing 0.2 M NaCl, 5 mM EDTA, 50 mM Tris-HCl (pH 7.5), 0.2% SDS and 400 µg/ml proteinase K. Genomic DNA was precipitated with ethanol, washed with 70% ethanol, air-dried and resuspended in H_20. For mouse tail biopsies, ~ 1 cm of tissue was digested overnight at 55°C in lysis buffer containing 200 µg/ml proteinase K, extracted with phenol/chloroform, and ethanol-precipitated as described above. To identify gene-targeted events and homozygote knockout mice, 5 µg of genomic DNA was digested with *Xba* I**,** and analyzed by Southern blot analysis. An 860 bp screening probe was generated by PCR using the primers Nat3 probe 5' and Nat3 probe 3' listed in Table 1 and 30 cycles of amplification consisting of 94˚C 10 s, 57˚C 10 s, 72˚C 30 s. The probe, corresponding to the region indicated in Fig. 1A, was labeled with [^{32}P]dCTP by random priming and hybridized overnight at 55˚C in ExpressHyb buffer (BD Biosciences Clontech, Mississauga, ON, Canada). The blots were washed 2 times in 2xSSC, 0.1%SDS, once in 0.2xSSC, 0.1% SDS and once in 0.1xSSC, 0.1% SDS for 15 min at 60˚C. Alternatively, an AlkPhos Direct™ labeling kit (GE Healthcare, Baie

D'urfe, QC, Canada) was used for the labeling and hybridization of the probe as per the manufacturer's instructions. A 3.1 kb band indicated the presence of the wild-type allele, whereas a targeted allele was evident as a 2.4 kb band upon digestion with *Xba* I.

For PCR genotyping of the mice, 100 ng of genomic DNA was subjected to PCR amplification in a 50 µl reaction volume (94˚C 30 s, 58˚C 30 s, 72˚C 45 s; 35 cycles). The wild-type allele was identified by amplification with the NAT3 5' primer and NAT3 3' primer. The targeted allele was amplified with the same forward NAT3 5' primer and the reverse primer PGKrev2 (see Table 1 for primer sequences), located within the *neo* cassette region.

Determination of *in vitro* NAT activity

Tissue cytosols were prepared from wild-type B6 and *Nat3*(-/-) animals as described (Sugamori et al., 2003). NAT activity for PAS, ABP and AF *N*-acetylation was determined using various tissue cytosols (n=3 per gender, genotype and tissue). Initial rates for the cytosolic fractions were performed in duplicate with 0.1 mM arylamine substrate, 0.1 mM acetyl-CoA and 20 µl regenerating system in a reaction volume of 100 µl. The regenerating system consisted of 5 mM acetyl-DL-carnitine and 1 U carnitine acetyltransferase per milliliter of assay buffer (250 mM triethanolamine-HCl, 5 mM EDTA, 5 mM dithiothreitol, pH 7.5). Reactions were preincubated for 3 min at 37°C and initiated with the addition of diluted cytosol at a protein concentration of 1 mg/ml. The reactions were incubated for 10 min at 37°C and terminated by the addition of 10 µl of 15% perchloric acid. After precipitation of the denatured protein, the supernatant fractions were assayed for the *N*-acetylated product (APAS, AABP or AAF) by HPLC using a Shimadzu LC-2010A System (Mandel Scientific Company Inc., Guelph, ON, Canada) and a reverse-phase Beckman Ultrasphere ODS 5 µM column (15 cm x 4.6 mm I.D.;

Beckman Instruments, Fullerton, CA). A flow rate of 2 ml/min with a mobile phase consisting of 66% sodium perchlorate buffer:34% acetonitrile and an ultraviolet detector setting of 280 nM were used for ABP- and AF-NAT activity assays. For PAS-NAT activity assays, a mobile phase consisting of 7% acetonitrile:1% acetic acid:0.1% triethylamine and an ultraviolet detector setting of 270 nM were used.

Drug administration and plasma elimination kinetics

PAS, ABP, AF or SMZ (50 mg/kg) dissolved in saline (PAS, SMZ) or DMSO (ABP, AF) was administered by intraperitoneal (i.p.) injection to 8-9 week old age-and sex-matched *Nat3*(-/-) mice and wild-type B6 mice (n=3 each). Blood samples were drawn from the saphenous vein using heparinized microvettes (Sarstedt Inc., Montreal, QC, Canada) at 4 different time-points (15 min, 30 min, 60 min, 90 min for PAS; 2 hr, 6 hr, 22 hr, 24 hr for ABP and SMZ; 1 hr, 2 hr, 4 hr, 6 hr for AF) and centrifuged to separate plasma. Plasma samples were diluted 1:50 in HPLC mobile phase, and analyzed for parent and acetylated products by HPLC as described above for the *in vitro* assays. For SMZ and ASMZ, a mobile phase consisting of 88% sodium perchlorate buffer:12% acetonitrile and an ultraviolet detector setting of 254 nM were used. Blank plasma samples were spiked with known amounts of parent and acetylated metabolites to quantify the amount of parent and acetylated products present in the samples. Area under the curve values (AUC) were determined by the trapezoidal rule using the computer program Prism (GraphPad Software Inc., San Diego, CA). Statistical analyses were performed using a Student's *t* test with GraphPad Prism.

RNA and RT-PCR

Total RNA was prepared using Trizol (Invitrogen) from various tissue sources (liver, kidney, colon, bladder, cerebral cortex, cerebellum and spleen). Approximately 1 µg of total RNA was treated with DNase for 30 min at 37˚C, heat-inactivated in the presence of 2.5 mM EDTA for 10 min at 65˚C, followed by reverse transcription using a RevertAid cDNA synthesis kit (MBI Fermentas, Burlington, ON) and oligo dT. Briefly, the RNA was incubated with 0.5 µg oligo dT for 5 min at 70˚C followed by addition of reaction buffer (50 mM Tris-HCl, pH 8.3, 50 mM KCl, 4 mM $MgCl_2$, 10 mM DTT), 20 u ribonuclease inhibitor and 200 µM dNTPs. The reaction was incubated for 5 min at 37˚C prior to the addition of 200 u of RevertAid^{TM} H Minus M-MuLV reverse transcriptase (RT) and incubation for 60 min at 42˚C. One-tenth volume of the RT reaction corresponding to 100 ng of total RNA was subjected to PCR amplification (94˚C 30 s, 56˚C 30 s, 72˚C 45 s; 35 cycles) with NAT3 and β-actin primers (listed in Table 1). For the strain-specific primers, the cycling conditions consisted of 35 cycles of 94˚C 10 s, 62˚C 10 s, 72˚C 45 s and as a positive control, reactions were performed with 100 ng of either CAST/Ei or 129/SvJ genomic DNA. For all RT-PCR experiments, a no-RT control in which a mock reaction was carried out in the absence of RT to control for genomic DNA contamination and a no-template control with RT to account for DNA contamination in the reagents were performed in parallel. In addition, β–actin primers spanning 2 introns were used as an additional genomic DNA control and to serve as a positive control. PCR amplification with the NAT3 primers and β-actin primers were run in parallel reactions using the same cDNA template source.

DMD Fast Forward. Published on April 2, 2007 as DOI: 10.1124/dmd.107.015396
This article has not been copyedited and formatted. The final version may differ from this version.

RESULTS

Generation of *Nat3*(-/-) mice

The targeted disruption of the mouse *Nat3* gene was achieved by insertion of the neomycin resistance gene into the *Kpn I* site located within ~480 bp of the *Nat3* coding sequence, thereby completely disrupting its function. Homologous recombinant clones with the correct targeting event were identified by Southern blot analysis using a probe designed in the 3' flanking region as shown in Fig. 1A. From 71 double-resistant ES colonies, 4 colonies showing the correct gene targeting event were identified. A total of six male and four female chimeric mice, distinguished by the ES cell-derived agouti color were generated by morula aggregation experiments. Germline transmission was observed in 2 of the 6 male animals. Mice carrying the targeted allele were genotyped by Southern blot analysis of *Xba* I-digested genomic DNA (Fig. 1B). The presence of the targeted allele was evident by the presence of a 2.4 kb band, whereas the wild-type allele was identified by a band of 3.1 kb. Alternatively, mice were genotyped by PCR (Fig. 1C).

Chimeric mice showing germline transmission were bred with C57BL/6 mice. Heterozygous mice (+/-) displayed normal viability and fertility, and were intercrossed to produce homozygous mutants. Mice homozygous for the disrupted alleles were born normally and appeared indistinguishable (appearance, mortality rate, reproductive capacity) from their wild-type littermates. In addition, there appeared to be no *in utero* lethality of the homozygous null mice as determined by their frequency of about 31% in litters from heterozygote crosses (+/+, 21 offspring; +/-, 39 offspring; -/-, 27 offspring), and gross pathological observations revealed no apparent abnormalities. *Nat3*(+/-) mice were backcrossed 10 times to C57BL/6 mice to generate the knockout on a congenic B6 background.

DMD Fast Forward. Published on April 2, 2007 as DOI: 10.1124/dmd.107.015396
This article has not been copyedited and formatted. The final version may differ from this version.

In vitro NAT activity

Nat3(-/-) mice displayed no difference in cytosolic NAT activity compared to wild-type B6 mice for a number of substrates in either liver, kidney or colon (Fig. 2). A previously observed gender difference in PAS, ABP and AF acetylation was noted in the kidney for both *Nat3*(-/-) and wild-type mice. Male kidney cytosols for both wild-type and *Nat3*(-/-) mice exhibited about a two-fold higher activity (Fig. 2; $p < 0.05$) than female kidney cytosols of both genotypes. No other tissues displayed a gender difference.

In vivo NAT activity

Similar to the *in vitro* results with the tissue cytosols, *Nat3*(-/-) mice displayed no difference compared to wild-type mice upon the *in vivo* administration of several arylamine substrates. AUC values for parent and acetylated metabolites were not significantly different between the wild-type and knockout animals (Table 2), indicating that acetylation was not impaired for these substrates in the *Nat3*(-/-) animals.

Nat3 expression in wild-type, *Nat*3(-/-) and *Nat1/2*(-/-) mice

RNA was isolated from wild-type and *Nat3*(-/-) mice and subjected to RT-PCR to confirm disruption of the *Nat3* gene. The RT-PCR detected only very low levels of Nat3 transcript in wild-type animals and most often only in cerebral cortex and cerebellum (Fig. 3). Nat3 transcript could sometimes be detected in other tissues (spleen, colon, kidney and bladder) in wild-type animals, but these results were not consistent between animals. However, no Nat3 transcript could be detected in any of the tissues from *Nat3*(-/-) mice. In contrast, RT-PCR results from *Nat1/2*(-/-) (Fig. 3) and *Nat1/2*(+/-) mice (data not shown) clearly and reliably

indicated a high level of Nat3 transcript in all tissues. To determine whether this augmented Nat3 transcript in *Nat1/2* null mice was due to a physiologically relevant compensatory mechanism or the possible effect of adjacent insertion of the PGK-*neo* gene cassette, a transcribed marker polymorphism strategy was used to distinguish between expression of the *Nat3* alleles in mice heterozygous for the insertion. 129/SvJ and C57BL/6 mice have wild-type *Nat3*1* sequence, whereas CAST/Ei mice possess the *Nat3*2* allele which contains several single nucleotide polymorphisms (Boukouvala et al., 2002). We used RT-PCR and strain- or allele-specific primers to distinguish between transcripts produced from the wild-type *Nat3*1* allele and the CAST *Nat3*2* allele in F1 129/CAST *Nat1/2*(+/-) animals (Fig. 4A). RT-PCR analysis indicated that the amplified Nat3 transcript was derived only from the 129/SvJ disrupted-allele and not from the allele from the CAST/Ei strain (Fig. 4B). No Nat3 amplification could be detected using the CAST/Ei-specific primer.

DMD Fast Forward. Published on April 2, 2007 as DOI: 10.1124/dmd.107.015396
This article has not been copyedited and formatted. The final version may differ from this version.

DISCUSSION

We have generated a *Nat3* knockout mouse model to provide insight into what role, if any, Nat3 plays in the mouse. Previous recombinant protein expression experiments have thus far indicated that only AF (Kelly and Sim, 1994) and 5-AS (Estrada-Rodgers et al., 1998) show any measurable *N*-acetylation by Nat3. In contrast, the recently cloned rat Nat3 displays both functional *N*- and *O*-acetylation activity for a number of substrates when expressed in a bacterial system (Walraven et al., 2006). However, determination of the relative functional contribution of Nat3-mediated acetylation to the whole animal is difficult to assess without subtype-selective substrates, since Nat3 activity could be masked by Nat1 or Nat2 activity. A knockout model completely lacking other endogenous NAT activities or lacking Nat3 may thus help to determine the relative contribution of Nat3 to overall NAT activity.

Nat3(-/-) mice appear normal with respect to growth and reproductive capacity. This is not an unexpected finding given that *Nat2*(-/-) and *Nat1/2*(-/-) mice are viable (Cornish et al., 2003; Sugamori et al., 2003), even though Nat2 is implicated in folate catabolism and is expressed early in development in the neural tube and heart (McQueen et al., 2003; Payton et al., 1999; Wakefield et al., 2005). This would indicate that none of the NATs are essential for development or physiological homeostasis, and is in keeping with the theme for many other drug metabolizing knockout animals in which no deleterious phenotypes have been observed in the absence of chemical challenge (Gonzalez and Kimura, 2003). Nevertheless, possible endogenous roles for NATs may yet be revealed by utilizing microarray approaches, as has been done with *Cyp1a2* knockout mice (Smith et al., 2003).

On the other hand, such knockout animals may serve as useful models to study pathways of drug metabolism, chemical toxicity and carcinogenesis (Gonzalez, 2003), and have revealed

some unexpected findings that contradict *in vitro* studies. For instance, *Cyp1a2* knockout mice do not display lower ABP-DNA adducts (Tsuneoka et al., 2003) nor protection against ABP-induced carcinogenesis (Kimura et al., 1999), despite efficient *in vitro N*-oxidation of this chemical to a more highly toxic hydroxylamine by Cyp1a2. Similarly, *Cyp1a1* knockout mice exhibit increased rather than decreased toxicity from benzo[*a*]pyrene exposure (Uno et al., 2004; Uno et al., 2001).

To determine whether *N*-acetylation activity is impaired in *Nat3*(-/-) mice, both *in vitro* activity assays using tissue cytosols and *in vivo* plasma elimination studies were performed. Our results indicate that there is no decrease in cytosolic NAT activity for a number of substrates in our *Nat3*(-/-) animals. The gender difference in kidney PAS, ABP and AF acetylation (Sugamori et al., 2006; Sugamori et al., 2003) was seen in both the wild-type and *Nat3*(-/-) mice. In addition, no difference in the *in vivo* plasma elimination of PAS, ABP, AF or SMZ was observed between *Nat3*(-/-) and wild-type mice. This concurs with the *in vivo* results seen with our *Nat1/2*(-/-) mice, in which we were unable to detect any acetylated metabolites in the knockout animals at the level of sensitivity of our assays (Sugamori et al., 2006; Sugamori et al., 2003). The presence of acetylated metabolites in mice lacking both Nat1 and Nat2 would have indicated possible *N*-acetylation by Nat3. We were also unable to detect any *in vitro* PAS, AF and ABP *N*-acetylation activity in a number of different tissues (liver, kidney, colon, spleen and cerebral cortex) from our *Nat1/2*(-/-) mice (Sugamori et al., 2006; Sugamori et al., 2003).

Using RT-PCR, no Nat3 transcript was detected in tissues from the *Nat3* knockout animals. In wild-type animals only very low levels of transcript could be seen in some tissues such as cerebral cortex and cerebellum, and occasionally in a few other tissues (spleen, bladder, kidney, colon). These results were variable from animal to animal, indicating that the method

employed may not be sensitive enough to reliably detect low levels of expression, and confirming the difficulty in assessing Nat3 expression in mice. To date, Nat3 transcript has only been identified by other investigators in spleen (Boukouvala et al., 2002). We were unable to detect any NAT activity that could be attributed to this enzyme in the spleens of animals lacking Nat1 and Nat2 function (Sugamori et al., 2006; Sugamori et al., 2003).

In marked contrast, RT-PCR detected markedly increased levels of Nat3 transcripts in all tissues from *Nat1/2*(-/-) and *Nat1/2*(-/+) animals. To determine whether this represented a compensatory change in these animals due to an impairment of Nat1 and Nat2 activity or an artifact created by the original gene targeting event, we used a polymorphic marker in the *Nat3* gene to distinguish whether only the *Nat3* gene downstream of the targeting event was subjected to this augmentation, or whether both alleles were affected. CAST/Ei mice display several SNPs in the coding region of *Nat3* (Boukouvala et al., 2002). Thus by breeding *Nat1/2*(+/-) mice on a 129/SvJ background to CAST/Ei *Nat1/2* (+/+) mice to generate F1 heterozygotes, it is possible to distinguish by an allele- or strain-specific PCR reaction whether one or both alleles show increased expression. Increased expression of both the CAST/Ei *Nat3*2* allele (with an intact *Nat1/2* gene region) and the allele representing the *Nat3*1* gene downstream of the disrupted *Nat1/2* gene in a F1 heterozygous animal would imply that the effect is a true transcriptional activation of the functional *Nat3* promoter, and not merely the presence of the strong constitutive promoter in the PGK-*neo* cassette targeted to the *Nat1/2* gene region that alters transcription of the *Nat3* gene, located approximately 45 kb downstream of *Nat2* (Boukouvala and Fakis, 2005). Since amplification detected only transcript from the targeted allele, the increase in Nat3 transcript appears to be due to a 'neighborhood' effect, either due to insertion of the PGK-*neo* cassette or to removal of ~ 9 kb of genomic sequence.

Such a 'neighborhood' effect has been shown in a number of other knockout mouse models. For instance, a reduction was seen in the expression of the *Cyp2a5* gene in *Cyp2g1* knockout animals (Zhuo et al., 2004) and bidirectional transcriptional activity of PGK-*neo* resulted in embryonic lethality in heterozygote multiple endocrine neoplasia type 1 (MEN1) chimeric knockout mice (Scacheri et al., 2001). Most often the PGK-*neo* cassette was found to affect neighboring genes when inserted within gene clusters or locus control regions, such as the myogenic regulator factor genes (Olson et al., 1996), β-like globin locus control region (Hug et al., 1996), the *Hox* gene cluster (Ren et al., 2002) and the granzyme B gene cluster (Pham et al., 1996). In most of these cases, downstream gene expression was found to be attenuated with the exception of *Hoxa*1 expression, which showed ectopic expression due to the generation of a *neo*-*Hoxa*1 fusion transcript when the PGK-*neo* cassette was inserted in the 3'-UTR of the *Hoxa2* gene (Ren et al., 2002). Removal of the PGK-*neo* cassette would help determine if the transcriptional effect is due to the presence of the selection cassette and not the result of removal of inhibitory regulatory elements or changes in the local chromatin structure due to deletion of almost 9 kb of genomic sequence. Regardless, the increase in Nat3 transcript in our *Nat1/2*(-/-) mice did not result in any functional change, since we were unable to detect any Nat3-mediated *N*-acetylation activity in these animals with prototypical NAT substrates. Our results suggest not only that Nat3 does not play a significant role in acetylating prototypical NAT arylamine substrates in the mouse, but that Nat3 transcript levels are not predictive of enzyme function. In this regard, it is possible that the *Nat3* gene is on the evolutionary path to becoming a pseudogene which is incapable of producing a functional product. However, other possibilities remain that Nat3 displays activity towards other as-yet discovered substrates, or that it performs a still unknown role in the mouse.

ACKNOWLEDGEMENTS

We thank Xiaoli Lu for valuable and excellent technical assistance.

REFERENCES

Boukouvala S and Fakis G (2005) Arylamine *N*-acetyltransferases: what we learn from genes and genomes. *Drug Metab Rev* **37**:511-564.

Boukouvala S, Price N and Sim E (2002) Identification and functional characterization of novel polymorphisms associated with the genes for arylamine *N*-acetyltransferases in mice. *Pharmacogenetics* **12**:385-394.

Boukouvala S and Sim E (2005) Structural analysis of the genes for human arylamine *N*-acetyltransferases and characterization of alternative transcripts. *Basic Clin Pharmacol Toxicol* **96**:343-351.

Cornish VA, Pinter K, Boukouvala S, Johnson N, Labrousse C, Payton M, Priddle H, Smith AJ and Sim E (2003) Generation and analysis of mice with a targeted disruption of the arylamine *N*-acetyltransferase type 2 gene. *Pharmacogenomics J* **3**:169-177.

Dupret JM, Goodfellow GH, Janezic SA and Grant DM (1994) Structure-function studies of human arylamine *N*-acetyltransferases NAT1 and NAT2. Functional analysis of recombinant NAT1/NAT2 chimeras expressed in *Escherichia coli*. *J Biol Chem* **269**:26830-26835.

Estrada-Rodgers L, Levy GN and Weber WW (1998) Substrate selectivity of mouse *N*-acetyltransferases 1, 2, and 3 expressed in COS-1 cells. *Drug Metab Dispos* **26**:502-505.

Fretland AJ, Doll MA, Gray K, Feng Y and Hein DW (1997) Cloning, sequencing, and recombinant expression of NAT1, NAT2, and NAT3 derived from the C3H/HeJ (rapid) and A/HeJ (slow) acetylator inbred mouse: functional characterization of the activation and deactivation of aromatic amine carcinogens. *Toxicol Appl Pharmacol* **142**:360-366.

Glowinski IB and Weber WW (1982) Genetic regulation of aromatic amine *N*-acetylation in inbred mice. *J Biol Chem* **257**:1424-1430.

Gonzalez FJ (2003) Role of gene knockout and transgenic mice in the study of xenobiotic metabolism. *Drug Metab Rev* **35**:319-335.

Gonzalez FJ and Kimura S (2003) Study of P450 function using gene knockout and transgenic mice. *Arch Biochem Biophys* **409**:153-158.

Grant DM, Goodfellow GH, Sugamori K and Durette K (2000) Pharmacogenetics of the human arylamine *N*-acetyltransferases. *Pharmacology* **61**:204-211.

Hein D (2002) Molecular genetics and function of NAT1 and NAT2: role in aromatic amine metabolism and carcinogenesis. *Mutat Res* **506-507**:65-77.

Hein DW (2006) *N*-acetyltransferase 2 genetic polymorphism: effects of carcinogen and haplotype on urinary bladder cancer risk. *Oncogene* **25**:1649-1658.

Hein DW, Doll MA, Fretland AJ, Gray K, Deitz AC, Feng Y, Jiang W, Rustan TD, Satran SL and Wilkie TR, Sr. (1997) Rodent models of the human acetylation polymorphism: comparisons of recombinant acetyltransferases. *Mutat Res* **376**:101-106.

Hug BA, Wesselschmidt RL, Fiering S, Bender MA, Epner E, Groudine M and Ley TJ (1996) Analysis of mice containing a targeted deletion of beta-globin locus control region 5' hypersensitive site 3. *Mol Cell Biol* **16**:2906-2912.

Kelly SL and Sim E (1994) Arylamine *N*-acetyltransferase in Balb/c mice: identification of a novel mouse isoenzyme by cloning and expression *in vitro*. *Biochem J* **302**:347-353.

Kim D and Guengerich FP (2005) Cytochrome P450 activation of arylamines and heterocyclic amines. *Annu Rev Pharmacol Toxicol* **45**:27-49.

Kimura S, Kawabe M, Ward JM, Morishima H, Kadlubar FF, Hammons GJ, Fernandez-Salguero P and Gonzalez FJ (1999) CYP1A2 is not the primary enzyme responsible for 4-aminobiphenyl-induced hepatocarcinogenesis in mice. *Carcinogenesis* **20**:1825-1830.

Levy GN and Weber WW (1989) 2-Aminofluorene-DNA adduct formation in acetylator congenic mouse lines. *Carcinogenesis* **10**:705-709.

Levy GN and Weber WW (1992) 2-Aminofluorene-DNA adducts in mouse urinary bladder: effect of age, sex and acetylator phenotype. *Carcinogenesis* **13**:159-164.

Martell KJ, Vatsis KP and Weber WW (1991) Molecular genetic basis of rapid and slow acetylation in mice. *Mol Pharmacol* **40**:218-227.

McQueen CA, Mitchell MK, Dang LN, Chau B, Tjalkens RB and Philbert MA (2003) Prenatal expression of *N*-acetyltransferases in C57Bl/6 mice. *Chem Biol Interact* **145**:77-87.

Nebert DW (2000) Drug-metabolizing enzymes, polymorphisms and interindividual response to environmental toxicants. *Clin Chem Lab Med* **38**:857-861.

Nebert DW (2006) Comparison of gene expression in cell culture to that in the intact animal: relevance to drugs and environmental toxicants. Focus on "development of a transactivator in hepatoma cells that allows expression of phase I, phase II, and chemical defense genes". *Am J Physiol Cell Physiol* **290**:C37-41.

Olson EN, Arnold HH, Rigby PW and Wold BJ (1996) Know your neighbors: three phenotypes in null mutants of the myogenic bHLH gene *MRF4*. *Cell* **85**:1-4.

Payton M, Smelt V, Upton A and Sim E (1999) A method for genotyping murine arylamine *N*-acetyltransferase type 2 (NAT2): a gene expressed in preimplantation embryonic stem cells encoding an enzyme acetylating the folate catabolite *p*-aminobenzoylglutamate. *Biochem Pharmacol* **58**:779-785.

Pham CT, MacIvor DM, Hug BA, Heusel JW and Ley TJ (1996) Long-range disruption of gene expression by a selectable marker cassette. *Proc Natl Acad Sci U S A* **93**:13090-13095.

Ren SY, Angrand PO and Rijli FM (2002) Targeted insertion results in a rhombomere 2-specific *Hoxa2* knockdown and ectopic activation of *Hoxa1* expression. *Dev Dyn* **225**:305-315.

Rothman N, Bhatnagar VK, Hayes RB, Zenser TV, Kashyap SK, Butler MA, Bell DA, Lakshmi V, Jaeger M, Kashyap R and et al. (1996) The impact of interindividual variation in NAT2 activity on benzidine urinary metabolites and urothelial DNA adducts in exposed workers. *Proc Natl Acad Sci U S A* **93**:5084-5089.

Scacheri PC, Crabtree JS, Novotny EA, Garrett-Beal L, Chen A, Edgemon KA, Marx SJ, Spiegel AM, Chandrasekharappa SC and Collins FS (2001) Bidirectional transcriptional activity of PGK-neomycin and unexpected embryonic lethality in heterozygote chimeric knockout mice. *Genesis* **30**:259-263.

Smith AG, Davies R, Dalton TP, Miller ML, Judah D, Riley J, Gant T and Nebert DW (2003) Intrinsic hepatic phenotype associated with the *Cyp1a2* gene as shown by cDNA expression microarray analysis of the knockout mouse. *EHP Toxicogenomics* **111**:45-51.

Sugamori KS, Brenneman D and Grant DM (2006) *In vivo* and *in vitro* metabolism of arylamine procarcinogens in acetyltransferase-deficient mice. *Drug Metab Dispos* **34**:1697-702.

Sugamori KS, Wong S, Gaedigk A, Yu V, Abramovici H, Rozmahel R and Grant DM (2003) Generation and functional characterization of arylamine *N*-acetyltransferase *Nat1/Nat2* double-knockout mice. *Mol Pharmacol* **64**:170-179.

Tsuneoka Y, Dalton TP, Miller ML, Clay CD, Shertzer HG, Talaska G, Medvedovic M and Nebert DW (2003) 4-aminobiphenyl-induced liver and urinary bladder DNA adduct formation in *Cyp1a2*(-/-) and *Cyp1a2*(+/+) mice. *J Natl Cancer Inst* **95**:1227-1237.

Tybulewicz VL, Crawford CE, Jackson PK, Bronson RT and Mulligan RC (1991) Neonatal lethality and lymphopenia in mice with a homozygous disruption of the *c-abl* proto-oncogene. *Cell* **65**:1153-1163.

Uno S, Dalton TP, Derkenne S, Curran CP, Miller ML, Shertzer HG and Nebert DW (2004) Oral exposure to benzo[*a*]pyrene in the mouse: detoxication by inducible cytochrome P450 is more important than metabolic activation. *Mol Pharmacol* **65**:1225-1237.

Uno S, Dalton TP, Shertzer HG, Genter MB, Warshawsky D, Talaska G and Nebert DW (2001) Benzo[*a*]pyrene-induced toxicity: paradoxical protection in *Cyp1a1*(-/-) knockout mice having increased hepatic BaP-DNA adduct levels. *Biochem Biophys Res Commun* **289**:1049-1056.

Wakefield L, Cornish V, Broackes-Carter F and Sim E (2005) Arylamine *N*-acetyltransferase 2 expression in the developing heart. *J Histochem Cytochem* **53**:583-592.

Walraven JM, Doll MA and Hein DW (2006) Identification and characterization of functional rat arylamine *N*-acetyltransferase 3: comparisons with rat arylamine *N*-acetyltransferases 1 and 2. *J Pharmacol Exp Ther* **319**: 369-375.

Zhuo X, Gu J, Behr MJ, Swiatek PJ, Cui H, Zhang QY, Xie Y, Collins DN and Ding X (2004) Targeted disruption of the olfactory mucosa-specific *Cyp2g1* gene: impact on acetaminophen toxicity in the lateral nasal gland, and tissue-selective effects on *Cyp2a5* expression. *J Pharmacol Exp Ther* **308**:719-728.

FOOTNOTES

This research was supported by an operating grant from the National Cancer Institute of Canada, with funding from the Canadian Cancer Society.

1. Present address: Division of Clinical Pharmacology and Experimental Therapeutics, Children's Mercy Hospital and Clinics, Kansas City MO 64108
2. Present address: Amgen Inc., Thousand Oaks CA 91320-1799
3. Present address: Department of Cellular and Molecular Medicine, University of Ottawa, Ottawa, Ontario K1H 8M5
4. Present address: London Regional Cancer Program, University of Western Ontario, London, Ontario N6A 4L6

Reprint requests should be addressed to: D.M. Grant, Ph.D.
Department of Pharmacology
University of Toronto
1 King's College Circle
Toronto, Ontario M5S 1A8
denis.grant@utoronto.ca

DMD Fast Forward. Published on April 2, 2007 as DOI: 10.1124/dmd.107.015396
This article has not been copyedited and formatted. The final version may differ from this version.

LEGENDS FOR FIGURES

Fig. 1. Targeted knockout of the mouse *Nat3* gene by homologous recombination. **A,** Schematic representation of the wild-type *Nat3* gene region, the targeting vector for disruption of the *Nat3* gene, and the predicted homologous recombinant locus or disrupted allele. Location of the probe used for genotyping ES cell colonies and mice is shown by the stars in the 3' flanking region. The wild-type allele yields a band of 3.1 kb when digested with *Xba* I, whereas the targeted allele is represented by a 2.4 kb band. *neo*, neomycin resistance gene. *hsv-tk*, herpes simplex virus thymidine kinase gene. Restriction endonuclease sites in parentheses were lost during cloning/ligation. **B,** Southern blot analysis of genomic DNA from tail clips from representative wild-type, heterozygous and null mice. Wild-type mice (+/+) display a single band of 3.1 kb. Heterozygotes (+/-) are demarcated by the presence of two bands of 3.1 and 2.4 kb, and null mice (-/-) display only the band at 2.4 kb. **C,** PCR genotyping from representative wild-type, heterozygous and null mice. Wild-type mice (+/+) are representative of a single band at 607 bp. Heterozygotes (+/-) are evident by the presence of 607 and 333 bp bands and null mice (-/-) have only the 333 bp band.

Fig. 2. Cytosolic *N*-acetylation rates from wild-type and *Nat3*(-/-) mice. Tissue cytosols from wild-type and *Nat3*(-/-) mice were assayed for NAT activity with either 0.1 mM PAS **(A),** 0.1 mM ABP **(B)** or 0.1 mM AF **(C)** in the presence of 0.1 mM acetyl-CoA as described in the Materials and Methods. Product formation rates represent the mean from n=3 wild-type or knockout animals.

DMD Fast Forward. Published on April 2, 2007 as DOI: 10.1124/dmd.107.015396
This article has not been copyedited and formatted. The final version may differ from this version.

Fig. 3. RT-PCR detection of Nat3 and β-actin transcripts in tissues from representative wild-type, *Nat3*(-/-) and *Nat1/2*(-/-) mice. In each of the lane pairs, the '+' lane is a PCR reaction after reverse transcription, whereas the '-' lane is a negative control in which PCR was performed after a mock reverse transcription reaction in which RT was omitted, to control for false positive signals caused by genomic DNA contamination. DEPC is a diethyl pyrocarbonate-treated water negative control.

Fig. 4. Strategy to determine whether the PGK-*neo* cassette increases Nat3 transcript. **A,** A transcribed marker polymorphism (SNP) was used to distinguish between *Nat3* alleles in mice heterozygous for that marker (*Nat3*). 129/SvJ mice have wild-type *Nat3*1* sequence; CAST mice have *Nat3*2* sequence. A 129 Sv/J *Nat1/2*(+/-) mouse was bred to a CAST/Ei mouse and F1 heterozygotes having one *Nat1/2* knocked out allele (-) carried by the 129 strain and one CAST allele (+) were identified by PCR genotyping. These F1 animals would be heterozygous for *Nat3* (*Nat3*1/Nat3*2*). Amplification of only the *Nat3*1* sequence carried by the disrupted 129 allele would indicate that the gene targeting event affected downstream transcription due to a 'neighborhood' effect. **B,** RT-PCR analysis was performed using either allele- or strain-specific primers that distinguishes between the 129 or CAST Nat3 transcripts. Genomic DNA isolated from CAST or 129 strain liver served as a positive control for the primer pairs. the '+' lane is a PCR reaction after reverse transcription, whereas the '-' lane is a negative control in which PCR was performed after a mock reverse transcription reaction in which RT was omitted, to control for false positive signals caused by genomic DNA contamination.

DMD Fast Forward. Published on April 2, 2007 as DOI: 10.1124/dmd.107.015396
This article has not been copyedited and formatted. The final version may differ from this version.

TABLE 1

PCR Primers

Primer	Orientation	Sequence (5' to 3')
Nat3/Kpn 5'	sense	GAATGGAACCTGGTACCTGG
Nat3/Kpn 3'	antisense	GGGGTACCAGCCCTGACATTG
Nat3 probe 5'	sense	CTTCCATTTGTCATCAGCTTAG
Nat3 probe 3'	antisense	TGGGACTCCATGGAGGCAAAG
Nat3 5'	sense	GCATTCCCATTTTCCTGCCAG
Nat3 3'	antisense	CTCAAGGCTTCTCAGTCTGTCACC
PGKrev2	antisense	CATTTGTCACGTCCTGCACGAC
CASTNat3 5'	sense	ACCACGAACGATTGAAGATTTCTG
129Nat3 5'	sense	ACCACGAACGATTGAAGATTTCCA
β-actin 5'	sense	GCTTCTTTGCAGCTCCTTCGTTG
β-actin 3'	antisense	TACATGGCTGGGGTGTTGAAGGTC

PCR primers were used to generate the Southern blotting screening probe, for PCR genotyping the *Nat3*(-/-) mice, and for RT-PCR of Nat3- and β-actin-specific products from the various tissue sources. Conditions used for PCR amplification are described in the text.

DMD Fast Forward. Published on April 2, 2007 as DOI: 10.1124/dmd.107.015396
This article has not been copyedited and formatted. The final version may differ from this version.

TABLE 2

AUC values (mmol min/l) for ABP, AF, PAS and SMZ elimination

	Male +/+	**Male -/-**	**Female +/+**	**Female -/-**
PAS	9.6±1.6	9.7±1.8	9.2±2.4	12.2±2.7
APAS	7.4±2.4	8.7±2.0	7.6±0.9	8.9±1.5
ABP	220±28	196±14	177±42	225±68
AABP	6.1±0.6	5.0±0.7	6.0±1.3	5.4±0.5
AF	41.8±8.8	47.6±3.2	85.0±5.3	86.1±1.3
AAF	3.8±0.9	4.2±1.0	6.7±0.9	7.4±0.7
SMZ	536±26	512±21	567±116	570±129
ASMZ	52.9±9.5	58.6±6.5	29.8±7.4	37.5±8.8

AUC values (mmol min l^{-1}, mean ± SD, n=3) were determined by the trapezoidal rule using GraphPad Prism software. PAS, SMZ, ABP or AF (50 mg/kg) was dosed by i.p. injection to age- and sex-matched wild-type and knockout mice. Four sequential blood samples were drawn and analyzed for parent and metabolite compounds as described under *Materials and Methods.*

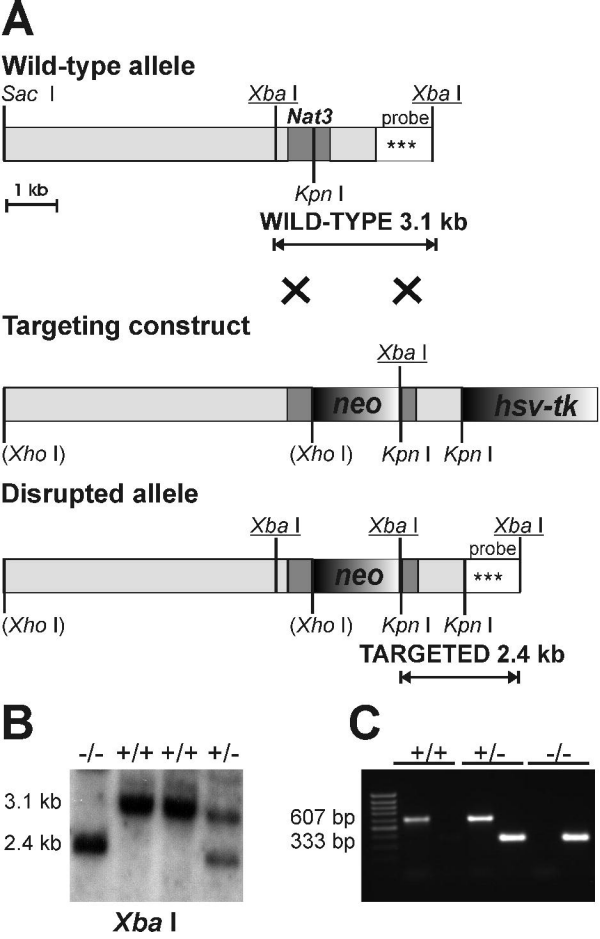
A
Wild-type allele
Sac I
Xba I
Nat3
Xba I
probe
***
1 kb
Kpn I
WILD-TYPE 3.1 kb
Targeting construct
Xba I
neo
hsv-tk
(Xho I)
(Xho I)
Kpn I
Kpn I
Disrupted allele
Xba I
Xba I
Xba I
probe
neo
***
(Xho I)
(Xho I)
Kpn I
Kpn I
TARGETED 2.4 kb
B
-/- +/+ +/+ +/-
3.1 kb
2.4 kb
Xba I
C
+/+
+/-
-/-
607 bp
333 bp

Fig. 1

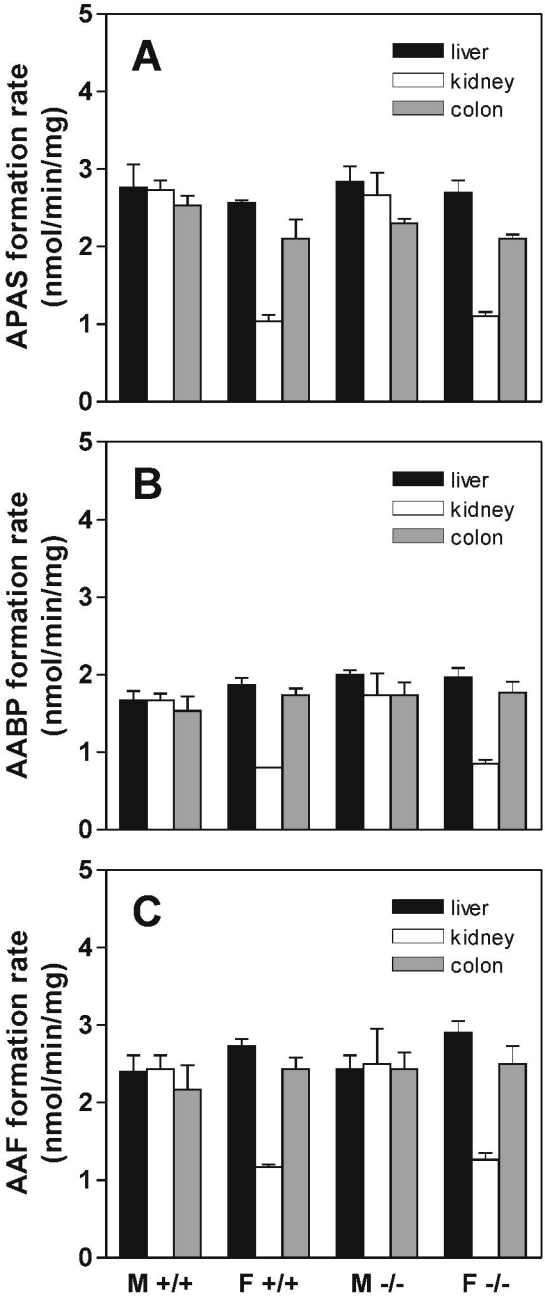
A
liver
kidney
colon
APAS formation rate
(nmol/min/mg)
0
1
2
3
4
5
B
liver
kidney
colon
AABP formation rate
(nmol/min/mg)
0
1
2
3
4
5
C
liver
kidney
colon
AAF formation rate
(nmol/min/mg)
0
1
2
3
4
5
M +/+
F +/+
M -/-
F -/-

Fig. 2

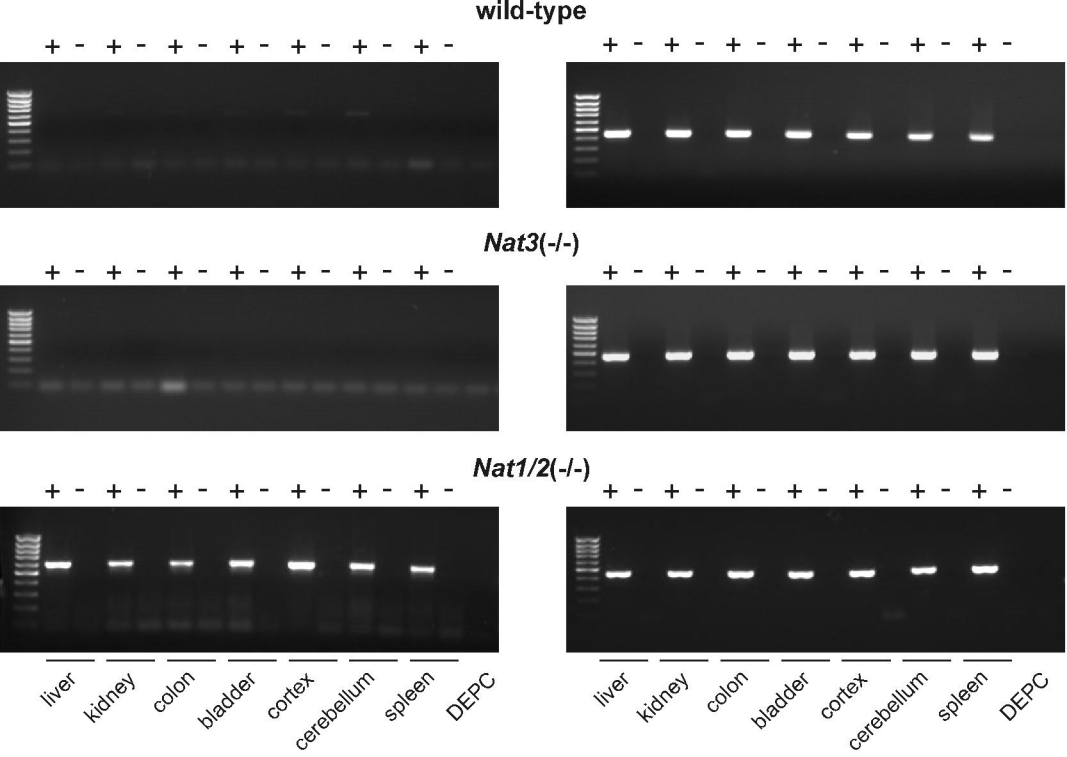
wild-type
+ - + - + - + - + - + - + -
+ - + - + - + - + - + - + -
Nat3(-/-)
+ - + - + - + - + - + - + -
+ - + - + - + - + - + - + -
Nat1/2(-/-)
+ - + - + - + - + - + - + -
+ - + - + - + - + - + - + -
liver
kidney
colon
bladder
cortex
cerebellum
spleen
DEPC
liver
kidney
colon
bladder
cortex
cerebellum
spleen
DEPC
mNAT3 607 bp
β-actin 448 bp

Fig. 3

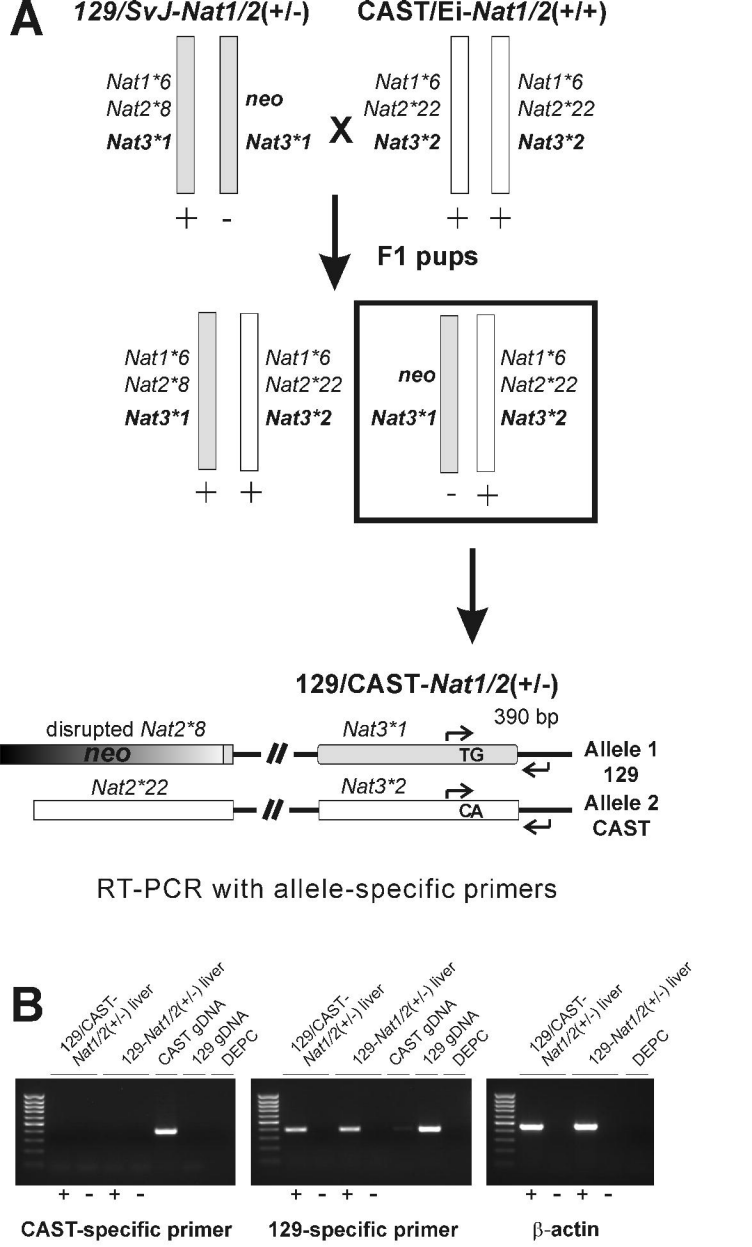
A
129/SvJ-Nat1/2(+/-)
CAST/Ei-Nat1/2(+/+)
Nat1*6
Nat2*8
Nat3*1
neo
Nat3*1
X
Nat1*6
Nat2*22
Nat3*2
Nat1*6
Nat2*22
Nat3*2
+ -
+ +
F1 pups
Nat1*6
Nat2*8
Nat3*1
Nat1*6
Nat2*22
Nat3*2
+ +
neo
Nat3*1
Nat1*6
Nat2*22
Nat3*2
- +
129/CAST-Nat1/2(+/-)
disrupted Nat2*8
neo
Nat3*1
390 bp
TG
Allele 1
129
Nat2*22
Nat3*2
CA
Allele 2
CAST
RT-PCR with allele-specific primers

B
129/CAST-Nat1/2(+/-) liver
129-Nat1/2(+/-) liver
CAST gDNA
129 gDNA
DEPC
+ - + -
CAST-specific primer
129-specific primer
β-actin

Fig. 4